



Article

Bodies and Glazes of Architectural Ceramics from the Ilkhanid Period at Takht-e Soleyman (North-Western Iran)

Stefan Röhrs ^{1,*} , Alexandra Dumazet ^{1,2}, Katharina Kuntz ^{3,4}  and Ute Franke ^{3,4}

¹ Rathgen-Forschungslabor, Staatliche Museen zu Berlin, Stiftung Preußischer Kulturbesitz, 14059 Berlin, Germany; alexandra.dumazet@culture.gouv.fr

² Centre de Recherche et des Restauration des Musées de France, Institut de Recherche de Chimie Paris, 75001 Paris, France

³ Institut für Vorderasiatische Archäologie, Freie Universität Berlin, 14195 Berlin, Germany; katharina.kuntz@fu-berlin.de (K.K.); ute_franke@yahoo.de (U.F.)

⁴ Museum für Islamische Kunst, Staatliche Museen zu Berlin, Stiftung Preußischer Kulturbesitz, 10117 Berlin, Germany

* Correspondence: s.roehrs@smb.spk-berlin.de

Abstract: Bodies and glazes of tiles from the Ilkhanid period found at the UNESCO World Heritage site of Takht-e Soleyman were studied to identify materials and certain technical characteristics of the architectural ceramics as part of a larger project to establish different productions. In addition, ceramic vessels and technical ceramics excavated at the site were analysed for comparison. μ XRF, SEM/EDX, and Raman spectroscopy were used for the material investigations. Qualitative non-invasive μ XRF results allowed for categorisation of the glazes and ceramic bodies based on their overall composition. Quantitative analysis by SEM/EDX on a subset of the samples delivered detailed results on the bodies and glazes. Tiles, made from clay or stonepaste, were almost exclusively decorated with a mixed alkaline lead glaze. The PbO content of this type of glaze ranged from 8 wt% to 25 wt%. The clay bodies of some tiles corresponded to the material of the locally used kiln furniture. Moreover, glaze residues preserved on the kiln furniture proved to be from a mixed lead alkaline glaze with a PbO content of 15 wt% to 25 wt%, a composition that is comparable to the tiles' glazes. For more insights into the local or regional production of the tiles, supplementary in-depth studies including petrographic analysis would be needed to confirm and further specify the results.

Keywords: ceramic body; glaze; cassiterite; colouring; XRF; SEM/EDX; Raman spectroscopy



Citation: Röhrs, S.; Dumazet, A.; Kuntz, K.; Franke, U. Bodies and Glazes of Architectural Ceramics from the Ilkhanid Period at Takht-e Soleyman (North-Western Iran). *Minerals* **2022**, *12*, 158. <https://doi.org/10.3390/min12020158>

Academic Editor: Domenico Miriello

Received: 17 November 2021

Accepted: 25 January 2022

Published: 27 January 2022

Publisher's Note: MDPI stays neutral with regard to jurisdictional claims in published maps and institutional affiliations.



Copyright: © 2022 by the authors. Licensee MDPI, Basel, Switzerland. This article is an open access article distributed under the terms and conditions of the Creative Commons Attribution (CC BY) license (<https://creativecommons.org/licenses/by/4.0/>).

1. Introduction

Located in north-western Iran, the site of Takht-e Soleyman, a UNESCO World Cultural Heritage site since 2003, hosts the remains of a Sasanian fire temple and a summer palace built by the Ilkhanid emperor Abaqa Khan in the second half of the 13th century. During the excavations conducted by the German Archaeological Institute, a large number of glazed ceramic tiles was found, indicating lavishly decorated buildings and interiors [1–6]. The Museum für Islamische Kunst in Berlin, Germany, houses a large collection of objects from Takht-e Soleyman thanks to a find division agreement and the subsequent transfer of the finds from the German Archaeological Institute to the Museum.

Tiles are generally classified technologically and stylistically according to fabrics of the body, form, and decorative techniques. This paper focusses on the analysis of fabrics and glazes from selected samples from Takht-e Soleyman. A full catalogue presenting the morphological types, their forming techniques, and the various types of decorative techniques is available in Franke 1979 [7]. An extended version in the final report on the Ilkhanid occupation of the site is in preparation [8]. General information on the typological range of shapes and decorative features of the tiles can be found in [9–11].

Their repertoire includes tiles with a flat surface or relief, with mono- or polychromatic glazes, different types of under-, on-, or in-glaze decorations, with or without lustre painting, and gilding. Although they have been scientifically studied from various perspectives [12–16], the question about their place of manufacture remains unresolved.

Gradman conducted a comprehensive study on Islamic architectural glazes including examples from Takht-e Soleyman kept in Berlin [12]. Based on electron probe microanalysis, she classified the glazes into two groups: an alkali group with less than 3 wt% PbO and a mixed group with an alkaline content and PbO ranging from 10 to 30 wt%. A third glaze group with a lead content of more than 55 wt% PbO was found on vessels [12]. This mixed alkaline lead group, widely studied on Islamic ceramic vessels, has an especially wide composition range. The PbO content is related to specific colours, but preferences of particular production areas and periods have also been observed [14,17–20]. An overview of the glaze compositions established by Gradmann [12] is given in Table 1; for each group, an average composition was calculated.

Table 1. Main oxide wt% average of glaze types with standard deviation for the three groups based on the results by Gradmann [12].

Type	SiO ₂	Al ₂ O ₃	PbO	MgO	CaO	Na ₂ O	K ₂ O	Fe ₂ O ₃
Alkali glazes	71.9 ± 6.9	4.0 ± 1.9	1.4 ± 1.1	1.2 ± 0.9	5.1 ± 1.5	11.5 ± 4.0	2.5 ± 0.5	2.1 ± 1.3
Mixed glazes	61.0 ± 7.2	1.7 ± 0.6	19.8 ± 5.1	0.6 ± 0.4	4.3 ± 1.1	7.3 ± 2.3	1.7 ± 0.4	1.3 ± 0.6
Lead glazes	32.9 ± 2.1	3.1 ± 0.2	59.6 ± 3.4	0.1 ± 0.1	1.4 ± 0.6	0.3 ± 0.1	0.5 ± 0.1	0.9 ± 0.6

Initial analysis of the ceramic bodies of eleven tiles from Takht-e Soleyman was carried out in 1978 by A. Kilb and in 1988 by G. Schneider by WDXRF in collaboration with U. Franke [7,8]. The fabrics were divided into chemical groups based on the following elements: clay bodies with low Si, high Fe, Ca, and Al, and silicate-rich stonepaste bodies with high Si and less Al, Ca, and Fe [16,21–25]. Based on this analysis, average compositions for the two different types of paste (clay and stonepaste) were calculated (Table 2).

Table 2. Average compositions of the two chemical body groups based on the results from G. Schneider in 1988; a brief description of the analytical technique can be found in [7,26].

Group	SiO ₂	TiO ₂	Al ₂ O ₃	Fe ₂ O ₃	MnO	MgO	CaO	Na ₂ O	K ₂ O
Group I: clay (N = 4)	58.57 ± 0.36	0.73 ± 0.02	15.91 ± 0.44	6.05 ± 0.19	0.15 ± 0.01	3.88 ± 0.14	9.75 ± 1.07	1.17 ± 0.04	3.52 ± 0.18
Group II: quartz (N = 7)	84.91 ± 2.51	1.02 ± 0.58	5.84 ± 1.35	1.04 ± 0.47	0.03 ± 0.01	1.13 ± 0.30	2.46 ± 0.99	2.43 ± 0.53	0.99 ± 0.24

Following the discovery of pottery kilns during the excavations, R. Naumann suggested in 1971 that glazed earthenware tiles and ceramic vessels were produced at the site [27]. However, establishing whether certain types of tiles were manufactured nearby or possibly imported from Kashan, presumably the leading ceramic workshop at the time [21], is a challenging goal of the analytical research. The differentiation of architectural ceramics into local production and imports would lead to a better understanding of the tile production processes needed for the large-scale construction programs of that time.

The present study focusses, in a first step, on the identification of the materials by a qualitative non-destructive XRF analysis that allows for the straight-forward classification of a large quantity of objects without sample preparation. Second, a more in-depth identification of the materials and of some of the tiles' technical characteristics was accomplished. The results were compared to vessels and kiln furniture excavated at the site; the latter related to local ceramic production.

2. Materials and Methods

2.1. Archaeological Material

Sixty-six artefacts, mainly architectural ceramics, from Takht-e Soleyman were studied. In addition, vessel fragments and material associated with ceramic production were

analysed. However, most of the vessels date from the 9th/10th to the 12th century, hence predating the Ilkhanid tiles. The production site of this pottery has also not been determined yet, but a large number of wasters from a specific type suggests a local or regional origin. The technical material mainly consists of kiln furniture such as rods used to support the ceramic during firing, tripods, and spacers. One fragment (K4, TS 1055) is a lump of vitrified glassy material of unknown purpose; possibly some sort of raw or waste material. The date of this technical equipment is unclear. Although the vessels and the technical elements are not necessarily contemporary with the tiles, they attest the applied technologies and raw materials available at the site. The complete list of the analysed artefacts is provided in the Supplementary Materials.

It has been observed that earthenware tiles are more weathered by environmental factors than stonepaste tiles. These were used in the interior whilst the clay tiles decorated the exterior walls [11,16]. Specific weathering products were observed on several of the tiles' glazes. For example, calcite on the glaze of sample P16 (TS861), detected by a strong Raman signal at 1086 cm^{-1} and corresponding weaker peaks, is probably a component of alteration and weathering. Calcite cannot withstand high firing temperatures (it disintegrates at $900\text{ }^{\circ}\text{C}$) or is digested by the glaze. In a study by Osete-Cortina et al., three stonepaste tiles with blue mixed alkaline glaze and apparent glaze corrosion layers were investigated [15]. The superficial alteration layer was found to have a $2\text{ }\mu\text{m}$ to $5\text{ }\mu\text{m}$ thickness and was recognizable by a significantly reduced Na_2O content below 4 wt%. An impact of possible weathering products on the analyses was avoided by the preparation of cross-sections for the quantitative analyses by SEM/EDX and the selection of appropriate areas.

The bodies of the tile collection in Berlin and the investigated samples have been macroscopically classified into the paste types of clay or stonepaste [7,16]. Under optical microscopy, the difference in terms of colour and mineralogical structure between these two principal body types, clay (I) and stonepaste (II; III), are clearly visible. The whitish stonepaste contains many aplastic inclusions, among them quartz from crushed pebbles. In the reddish clay fabric, inclusions were smaller and present in lower amounts. Stylistic features and decorative techniques led to a further classification of the tiles. Roman numerals are used to label groups defined by fabric; the stonepaste group was further differentiated by the presence resp. absence of lustre painting (II, III). The subsequent letters indicate the applied forming and decorative techniques:

- I: clay body, unglazed, partially, or fully glazed
 - IA: relief decoration
 - IB: flat decoration
- II: stonepaste body
 - IIA: flat surface, monochromatic glaze
 - IIB: relief surface, monochromatic glaze
 - IIC: flat or relief (moulded) surface, onglaze decoration (incl. lajvardina)
 - IID: relief (moulded) surface, under- and onglaze decoration
- III: stonepaste body, with lustre painting
 - IIIA: relief (moulded) surface
 - IIIB: flat surface

The subsequent upper-case letter, followed by a running number, specifies the object type of the sample:

- K: kiln furniture or technical material
- M: fragments of tiles where only one glaze colour was analysed
- P: fragments of tiles where multiple glaze colours were analysed
- U: tiles without glaze
- V: vessel sherd (for comparison)

For the qualitative XRF analysis, the lower-case letters indicate the glaze colour of the area analysed:

- w: white

- b: blue
- t: turquoise
- g: green
- y: yellow
- m: brown
- p: purple
- bk: black

2.2. Analytical Methods

2.2.1. Optical Microscopy

Objects were documented using a Zeiss Discovery V8 zoom microscope. Photos were taken with a digital camera from Jenoptik-ProgRes CFcool (1360 × 1024 pixel).

2.2.2. XRF Measurements

Samples without a fresh clean break exposing unaltered material were either cut with the diamond blade of a circular saw or the weathered surface was removed with a rotating polishing tool.

An ARTAXTM (Bruker AXS Microanalysis GmbH, Berlin, Germany) with a Mo X-ray tube was used. For the glazes, several measurements (at least two) were performed for each glaze colour. All measurements lasted 100 s live time and covered an area of 0.0079 mm² (45 kV, 500 µA, under He atmosphere, no filter, 50 keV). Line scans were performed on the body of each sample, whereby the line was chosen randomly to represent the macroscopic inhomogeneity of the paste. Each scan consisted of 10 measurements of 20 s. Data were processed on the Spectra 7 software (Bruker AXS Microanalysis GmbH, Berlin, Germany); for the line scans of the bodies, results were averaged over all ten measurements.

The XRF data are presented in counts: the number of counts obtained for a given element was normalized by the total number of counts in the spectrum to compensate for variations in the sample's geometry. The obtained values were then multiplied by 100 to obtain more readable numbers with less decimals.

2.2.3. ESEM/EDX

Sampling was necessary for the electron microscope analysis of the bodies and glazes of the sherds. Small pieces were embedded in epoxy resin, sanded, and polished with 3 µm diamond paste. A detailed investigation of the polished surface in connection with the possibility of elemental analysis was performed with the scanning electron microscope Quanta 200 (FEI, Hillsboro, United States) with a W-cathode. The instrument was used in low vacuum mode, which did not require conductive coating of the samples.

The X-rays are registered by a dispersive energy X-ray detector X Flash 4010 (Bruker AXS Microanalysis GmbH, Berlin, Germany). The electron microscope was calibrated with a copper sample to determine the current of the electron beam. The accuracy of the quantification was verified by the analysis of three glass samples with known composition from the Corning Museum of Glass (Corning glass A, B, and C) [28]. The results are available in the Supplementary Materials.

Samples were studied at a 0.3 mbar pressure of H₂O atmosphere and with electrons at 20 keV at a beam width set to 7 (maximum). Each sample, from glaze or body, was subject to at least one map-scan for quantification. The area of the mapping depended on the size of the sample and was selected to include representative material heterogeneities. Results were processed with the Bruker Esprit 1.9 software using a Phi-Rho-Z quantification method. The limit of quantification is about 0.1 wt% for transition metals.

2.2.4. Raman Spectroscopy

The Raman spectra were acquired with a XploRa Raman microscope (Horiba, Kyōto, Japan) fitted with lasers with wavelengths of 532 nm, 638 nm, and 785 nm. The powers of the respective lasers were 25 mW (532 nm), 24 mW (638 nm), and 90 mW (785 nm). Most

measurements were made with a 50× long working distance objective. The filter setting and acquisition times were adjusted to optimize the measured spectrum.

3. Results and Discussion

3.1. Classification of Materials by Non-Invasive μ -XRF

3.1.1. Bodies

Non-invasive semi-quantitative XRF analysis was used to study all bodies. The goal was to characterize groups by ceramic paste to reduce the number of invasive analyses by ESEM/EDX, which requires sampling. The XRF analyses of the 65 ceramics was carried out in a non-destructive approach. The counts of the four elements Al, Si, Ca, and Fe were used as variables in a hierarchical cluster analysis (Ward's method) to distinguish between stoneware and earthenware. The chosen elements reflect the different materials: for stoneware, the traditional recipe includes 10 parts quartz, one part glass, and only one part clay [22], whereas the earthenware or clay tiles have a content of over 40% clay [16,17].

All but one tile matched with the group determined by macroscopic observation (I: clay tiles, II and III: stoneware). One sample was visually classified as stoneware group IIB, M1 (TS1093.1), plots within the clay cluster, as confirmed by the subsequent quantitative analysis by SEM/EDS. All bodies of the kiln furniture and vessels (except the stoneware sherd V3/ISL11) were in the clay cluster.

3.1.2. Glazes

For the classification of the glazes, the same approach as for the bodies was adopted. Non-invasive XRF analysis was applied to reduce the number of invasive ESEM/EDX on the glazes. In total, 102 measurements were taken of 60 objects with glaze; objects with several colours were measured more than once. A clear division of the glazes into compositional groups based on the Si, K, Ca, and Pb XRF counts was possible. The results of a hierarchical cluster analysis (Ward's method) are shown in Figure 1. Due to the high sensitivity of the XRF for lead, the variation in lead content produced large distances. The separation of the data as presented in the dendrogram into three clusters resulted in groups corresponding with the compositional grouping (lead, mixed alkaline lead, and alkaline glazes). The clustering was further verified by comparison with the results published by Gradmann for the same fragments. The later SEM/EDX results, shown in Table 8, also confirm the clustering. An exception is sample K1t, which was found to be a mixed alkaline lead glaze by SEM/EDX, instead of an alkaline glaze.

In summary, five objects showed alkaline glazes (tiles M14, M17, P2, P12, and vessel V3); ten vessels and one kiln furniture object (K2) had lead glazes; and 45 objects including sample K4, which was not categorised as glaze, belonged to the mixed alkaline lead group.

3.2. Analysis of the Ceramic Bodies

The bodies of 40 objects were studied by SEM/EDX analysis. These were selected based on their chemical and macroscopical grouping. The quantitative data are shown in Tables 3–7. The results are in accordance with the results from Schneider (Table 2). One clay sherd previously analysed by Gradmann (V2, ISL13) had slightly different results where we found lower Al_2O_3 values, which seems to be coherent with data from other vessel fragments and fits well into our group.

The quantitative SEM/EDX data could reproduce the XRF grouping and provided quantitative data for the clay and stoneware bodies. The EDX analysis of M1 (TS 1093.1, group IIB) confirmed the μ -XRF results and the grouping of the object into the clay group. However, the yellowish colour of this sample is singular since the other analysed earthenware fragments had a rather reddish fabric.

Generally, the ceramic pastes can be divided into three types: stoneware, calcareous, and non-calcareous clay bodies. These classifications are usually applied to Islamic ceramics [17]. Stoneware commonly shows a composition of >75 wt% SiO_2 , <8 wt% Al_2O_3 , and <9 wt% CaO. The CaO content allows us to differentiate between calcareous clay

bodies, which contain more than 6 wt% of CaO and more than (about) 6 wt% Al₂O₃, and non-calcareous clay bodies with less than 6 wt% CaO and more than 12 wt% Al₂O₃. All clay bodies analysed belonged to the calcareous clay type, which is by far the most common type from this area (Table 4) [17,20]. However, the CaO content of the bodies from Takht-e Soleyman was approximately 10 wt%, which is relatively low.

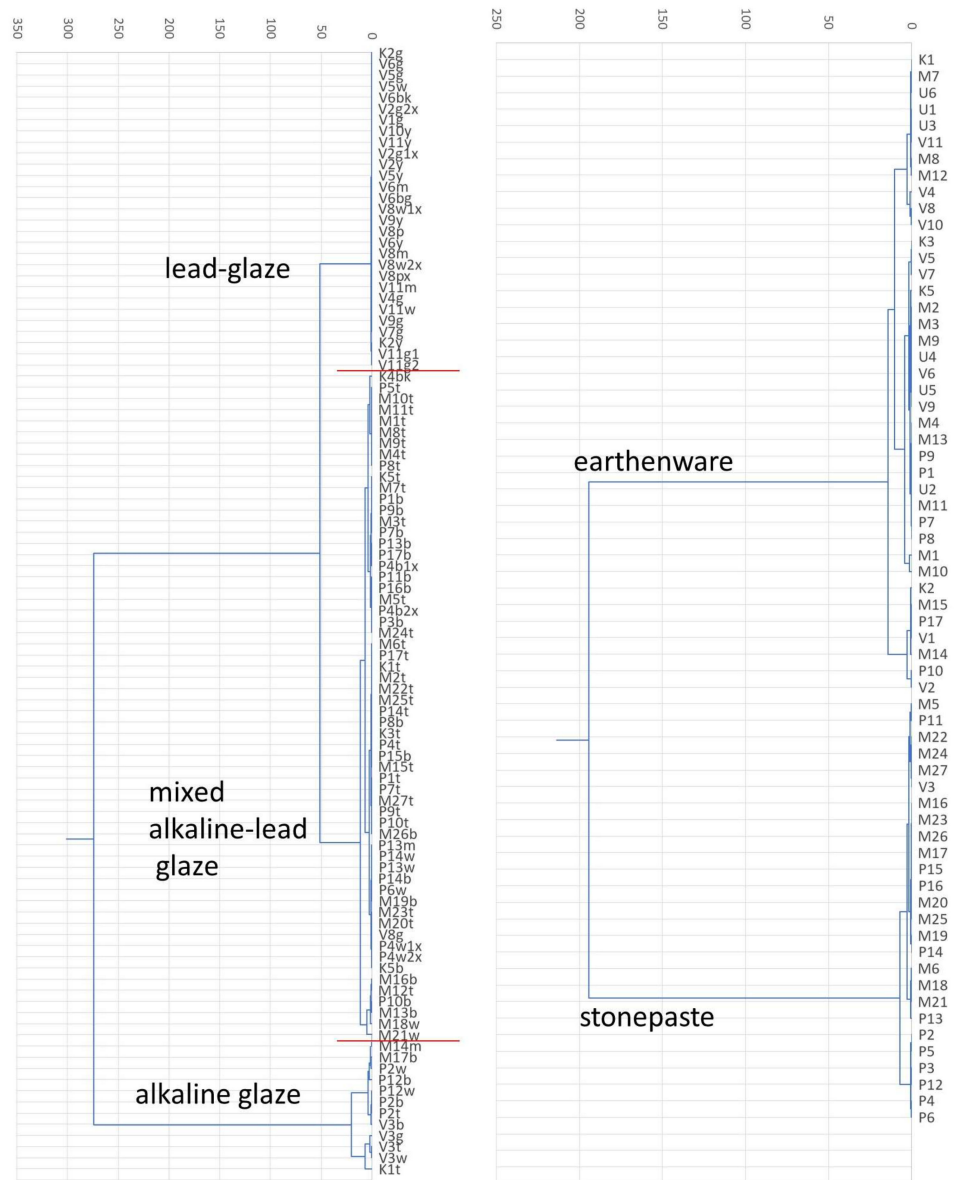


Figure 1. Dendrograms of cluster analyses of glazes and bodies based on qualitative XRF analysis.

Table 3. SEM/EDX results in wt% for the studied stonepaste bodies of tiles (N = 19).

	Na ₂ O	MgO	Al ₂ O ₃	SiO ₂	P ₂ O ₅	SO ₃	Cl	K ₂ O	CaO	TiO ₂	MnO	Fe ₂ O ₃	CuO	PbO
Average	3.0	1.2	5.8	78.9	0.5	2.2	0.4	1.7	2.3	1.5	0.1	1.1	0.1	1.0
Std. Dev.	0.7	0.4	1.3	3.6	0.2	2.4	0.1	0.4	0.8	0.7	0.0	0.4	0.1	1.0

Table 4. SEM/EDX results in wt% for the studied clay bodies of tiles (N = 13).

	Na ₂ O	MgO	Al ₂ O ₃	SiO ₂	P ₂ O ₅	SO ₃	Cl	K ₂ O	CaO	TiO ₂	MnO	Fe ₂ O ₃	CuO	PbO
Average	2.3	3.6	13.9	56.4	0.4	2.7	0.2	3.1	9.7	0.5	0.1	5.7	0.2	0.6
Std. Dev.	1.3	0.9	2.6	3.3	0.1	3.9	0.1	0.9	3.1	0.2	0.0	1.5	0.1	0.8

The average values of the two major compositional types were summarized according to object type: stonepaste tiles (Table 3), clay tiles (Table 4), stonepaste vessels (Table 5), clay vessels (Table 6), and kiln furniture (Table 7). A part of the chloride and sulphide content was considered as a later incorporation and not an initial component of the paste. The corresponding salts have possibly migrated into the paste during deposition in the ground [29], or from surrounding building materials (e.g., mortar).

Table 5. SEM/EDX results in wt% for the studied stonepaste body of vessel ($N = 1$).

	Na ₂ O	MgO	Al ₂ O ₃	SiO ₂	P ₂ O ₅	SO ₃	Cl	K ₂ O	CaO	TiO ₂	MnO	Fe ₂ O ₃	CuO	PbO
V3	2.9	1.5	3.8	85.5	0.3	0.4	0.3	1.8	1.5	0.2	<loq	1.3	<loq	<loq

Table 6. SEM/EDX results in wt% for the studied clay bodies of vessels ($N = 4$).

	Na ₂ O	MgO	Al ₂ O ₃	SiO ₂	P ₂ O ₅	SO ₃	Cl	K ₂ O	CaO	TiO ₂	MnO	Fe ₂ O ₃	CuO	PbO
Average	1.1	4.4	14.4	50.6	0.4	2.5	0.2	4.3	10.4	0.9	0.1	8.1	0.1	2.1
Std. Dev.	0.4	1.0	1.2	3.4	0.1	2.2	0.1	0.6	1.4	0.2	0.1	0.8	0.1	1.8

Table 7. SEM/EDX results in wt% for the studied bodies of the technical ceramic ($N = 3$).

	Na ₂ O	MgO	Al ₂ O ₃	SiO ₂	P ₂ O ₅	SO ₃	Cl	K ₂ O	CaO	TiO ₂	MnO	Fe ₂ O ₃	CuO	PbO
Average	3.8	4.7	13.1	51.9	0.5	3.6	0.2	3.7	8.3	0.6	0.1	6.8	0.3	1.8
Std. Dev.	0.3	0.4	1.0	1.2	0.3	1.8	0.0	1.0	0.5	0.2	0.0	0.7	0.2	0.6

The sulphur (probably as sulphates) content within the tiles was particularly variable and reached high values up to 7 wt% SO₃. The migration of the sulphur into the paste could be observed by SEM/EDX investigation, which showed that the sulphur was mainly localized in the voids of the ceramic.

A comparison of the results from clay bodies grouped by functionality revealed slight variances in the composition of tiles, vessels, and technical ceramics; however, a separation into individual groups is not possible. The tiles showed the highest average value of SiO₂ (Table 4). On average, vessels had the lowest SiO₂ and the highest iron content. Only a few tiles had an iron content of 5.5–9 wt% Fe₂O₃ and were in the same range as the vessels and the technical ceramics. The variation in composition might reflect differences in raw materials and/or clay processing.

The clay bodies were mostly made from dense red clay (Figure 2). The composition of the paste was characterized by a CaO content of around 10 wt%, which sets this production apart from the clay bodies with higher CaO contents from Mesopotamia or the Levant [14,20,30]. A higher compositional similarity of the clay bodies from Takht-e Soleyman can be found with clay objects from north-western Iran and Central Asia, as studies by Mason and Matin (including four sherds from Takht-e Soleyman) suggest. Although the number of analyses is limited, the materials found in Nishapur, Merv, and one object of the Garrus group are all in a similar compositional range of 53–62 wt% SiO₂, 13–15 wt% Al₂O₃, 2.5–5 wt% Mg, 0.7–15 wt% CaO, and 4.7–7 wt% Fe₂O₃ [14,20].

The stonepaste bodies had a SiO₂ content ranging from about 72 wt% to 85 wt% and Fe₂O₃ from <1 to 2 wt% (Figure 3). Tentatively, the distribution of the elements Si and Fe as well as other elements (Table 3) might suggest the use of at least two technologies: the first is a stonepaste (mainly) from quartz with the addition of glass, and the second is a stonepaste with a lower amount of SiO₂ and higher Na₂O, Al₂O₃, and Fe₂O₃, caused by a comparatively higher proportion of added clay [20,22]. The production of ceramics with a reduced SiO₂ content has been attributed to Kashan [20]. Lustre ceramic vessels from the Louvre Museum, dating from the pre-Mongol (1038–1194, 12 objects) and the Mongol-Period (1256–1353, 10 objects), studied by Chabanne et al. [29], have on average 77.5–78 wt% SiO₂ and 1–2 wt% Fe₂O₃. They are hence relatively similar in composition to

the type III tiles analysed in this study, but different to the lustre tiles analysed by Schneider. However, when comparing the values of the previous research and of this study, it must be considered that analytical methods (WD-XRF, PIXE, and SEM/EDX) with different analytical characteristics were used.

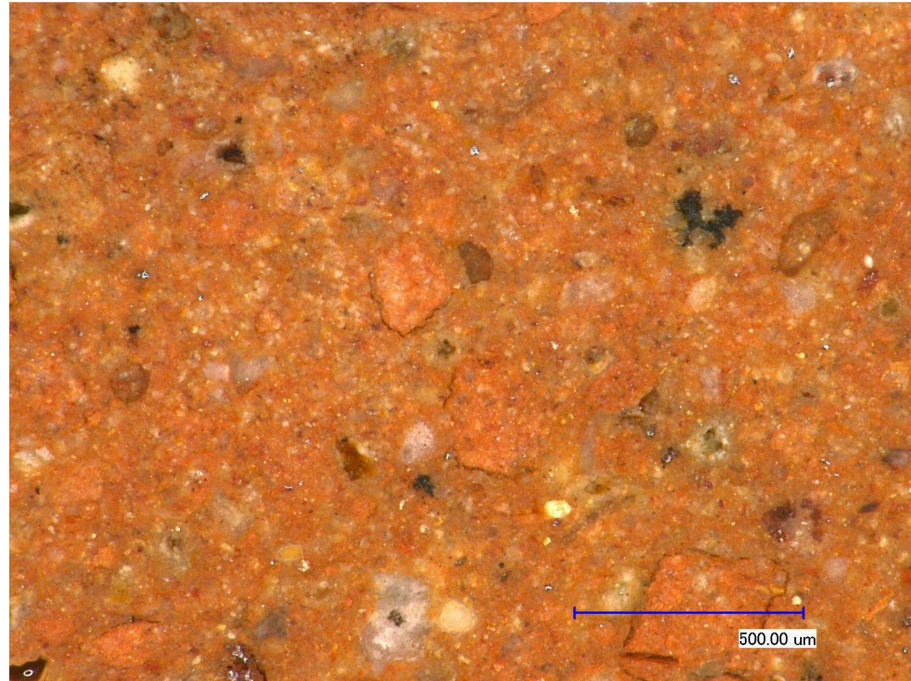


Figure 2. Micrograph of sample M15 (I.13/69.13A1).

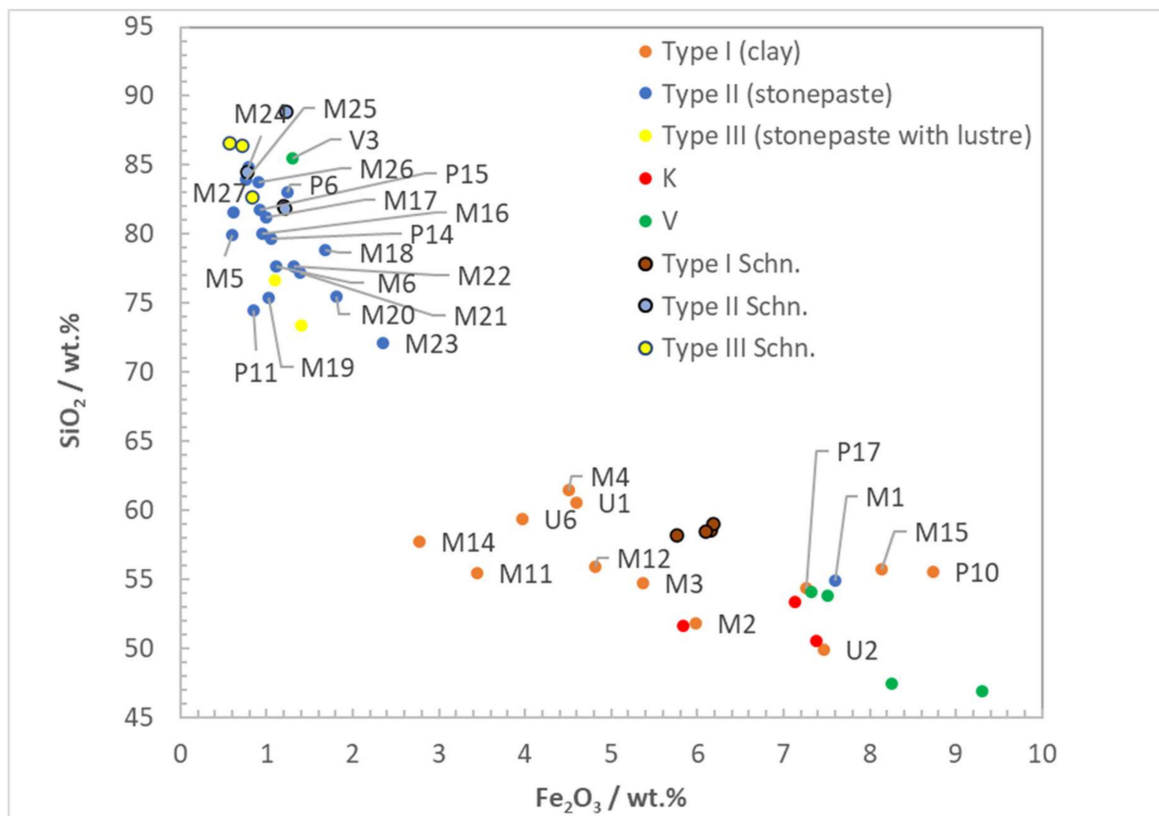


Figure 3. Scatter plot of SiO₂ and Fe₂O₃ for the ceramic bodies analysed by SEM/EDX. Analyses carried out by Schneider in 1988 are labelled with “Schn.” (Table 2).

Several cross-sections have been studied in more detail and were classified by their microstructure, as proposed by Tite et al. [23]. The stonepaste group II tiles without lustre decoration (P11, P14, P15, M20, M21, M22, M27) had a type 2 microstructure with glass fragments still present as inter-particles, indicating that during firing, the reaction with quartz has just started (Figure 4). The sizes of the quartz particles vary widely with a maximum of 200/250 μm in diameter. M21 (Type IIA) has different and coarser (up to 500 μm in diameter) types of particles; they also differ in shape by being more angular.

The overall PbO_2 content in the stonepaste ceramic was about 1 wt% (Tables 3 and S6) due to the glass particles. In some of the glass particles, tin-rich inclusions can be observed, suggesting that the glass is, at least partly, glazed with a tin opacifier.

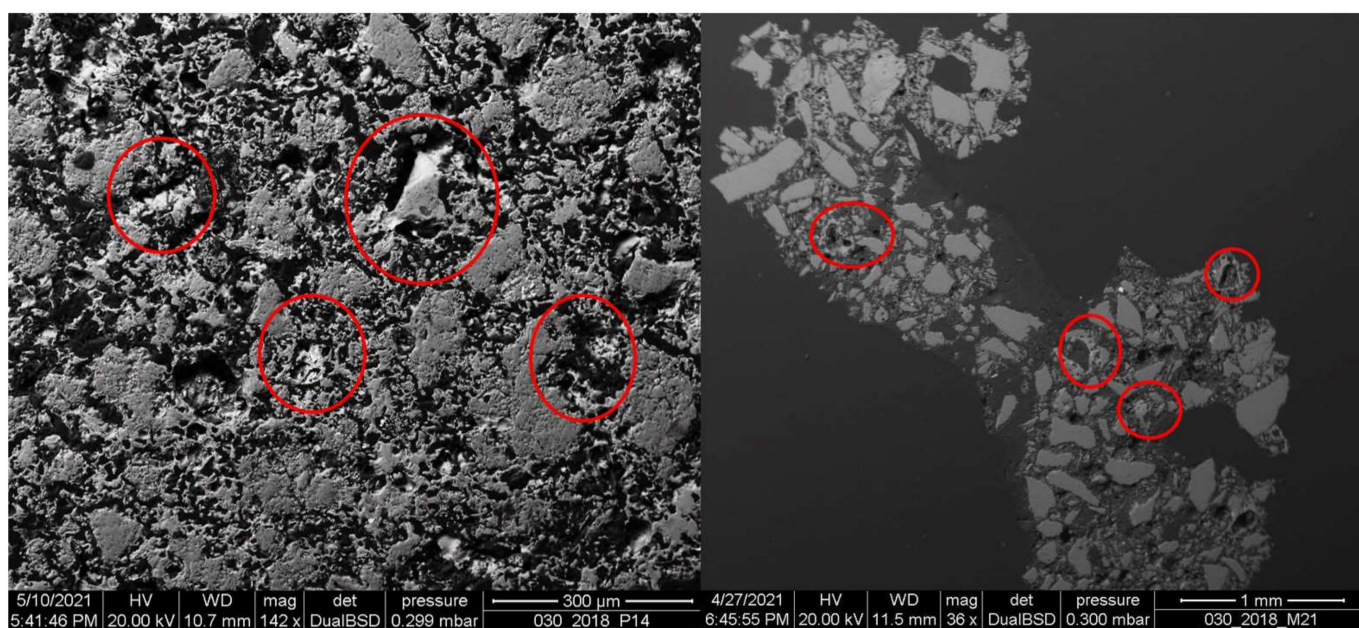


Figure 4. Back scatter electron images; glass particles in red circles. (Left) P14 (polychrome tile I. 4/67,24, group IID3c). (Right) M21 (monochrome tile ISL 7, group IIA).

3.3. Investigation of the Glazes

SEM/EDX analysis was performed on 28 objects. Two of the samples were previously already analysed by Gradmann [12], and the analytical results are compared in the Supplementary Materials. Some variation between our and the previous results was observed, but was of no significance for the grouping of the glazes. The SEM-EDX analysis confirmed the findings of the clustering from Figure 1. Most of the compositions fell into the group of mixed lead alkali glazes, as shown in Table 8.

The result of sample K4 (TS1055), which is a technical material of unknown function, did not match any of the glaze compositions. The sample was a dark, glassy object without the remains of a ceramic body. The material was richer in ZnO (7.2 wt%) and Fe_2O_3 (11.5 wt%) than all the other glaze samples, but had no significant CuO content. Therefore, it is not considered as a glaze, but rather as a raw or waste material. In the case of a raw material, the purpose of a zinc-rich precursor material is not apparent. Zn does not have glass colouring properties, but has an effect as a network modifier and could therefore have an influence on the colour of other colouring ions [31]. The ZnO found by XRF in the green glazes and in the black colour of P14 (TS09/IID) is probably only a trace, introduced to the glaze by the copper source.

Almost all glazes analysed by SEM/EDX belonged to the mixed group. Only samples M17 and V3 (alkali) and vessel objects V2, V4, V7, and V8 (lead) were different. The compositions of the mixed lead alkali glazes are summarised in Table 9. Especially for lead, the results showed a large variation. The PbO content was between 8.6 wt% to 25 wt%

(Figure 5), while the SnO₂ content to opacify the glazes was <10 wt%. This is in contrast to the observation made by Kaczmarczyk on ceramics from Susa from the 12th to the 14th century, which are predominantly alkaline glazes and not opacified [17]. In general, the alkaline content is reduced as the lead content increases. An overview of the analytical data classified by colour and glaze type is given in Table S6. The lead content within glazes is known to be related to colour (e.g., the lead content in white glazes is on average higher than in blue glazes) [18]. Turquoise glazes showed the highest variation in lead content. The turquoise glazes dropped from the technical (K1, K3 and K5) were all in the range of a high lead content, between 15 wt% and 25 wt% PbO.

Table 8. SEM/EDX results in wt% for the glazes, “<loq” indicates the compound was below the detection limit.

Sample	col.	Na ₂ O	MgO	Al ₂ O ₃	SiO ₂	P ₂ O ₅	SO ₃	Cl	K ₂ O	CaO	TiO ₂	MnO	Fe ₂ O ₃	CoO	CuO	ZnO	SnO ₂	PbO	Type
K1	T	6.2	1.5	4.5	57.3	0.1	<loq	0.4	3.4	3.4	0.2	<loq	2.0	<loq	1.2	0.0	3.7	15.4	M
K3	T	6.0	2.5	3.1	48.4	<loq	<loq	0.5	2.1	5.1	0.2	<loq	1.6	<loq	2.2	0.1	4.0	23.8	M
K4	B	1.0	1.2	5.9	40.4	0.2	<loq	0.1	1.7	5.5	0.6	0.8	11.5	0.1	0.2	7.2	<loq	20.2	-
K5	T	5.5	2.0	2.3	49.4	0.2	0.3	0.7	3.5	4.5	0.1	0.1	1.9	0.2	2.0	0.1	6.9	18.5	M
M3	T	6.5	2.0	1.9	51.3	<loq	<loq	0.7	2.0	3.5	0.1	0.1	0.8	0.1	2.4	<loq	5.5	22.3	M
M10	T	5.8	1.8	3.0	57.7	0.3	<loq	0.2	3.0	5.0	0.2	0.1	1.5	0.1	1.3	0.1	10.0	8.6	M
M11	T	4.2	2.1	2.7	56.5	0.1	0.5	0.3	3.2	4.3	0.1	<loq	1.2	<loq	1.5	0.2	5.7	16.0	M
M12	T	10.9	2.5	2.4	59.7	0.1	<loq	0.7	2.0	5.2	0.1	0.1	1.2	<loq	2.2	0.1	3.6	9.0	M
M15	T	6.5	1.7	1.7	50.4	<loq	<loq	0.6	1.7	3.4	0.1	<loq	1.4	<loq	2.4	0.3	6.3	22.3	M
M16	B	10.6	2.0	1.9	61.2	0.1	<loq	0.4	2.2	4.5	0.1	<loq	1.6	0.5	<loq	<loq	4.3	9.5	M
M17	B	14.0	2.8	2.9	65.9	0.3	0.1	0.4	2.2	6.6	0.2	<loq	2.3	0.3	<loq	<loq	0.4	1.2	A
M18	W	7.5	2.1	2.2	49.3	0.1	<loq	0.6	1.6	3.5	0.0	<loq	0.7	<loq	<loq	<loq	7.4	23.7	M
M19	B	8.3	2.2	1.7	55.1	0.1	<loq	0.5	1.1	3.4	0.1	<loq	1.6	0.6	0.1	<loq	6.7	17.0	M
M21	W	7.6	2.1	1.8	51.5	<loq	<loq	0.8	1.8	3.2	<loq	<loq	0.7	<loq	0.0	<loq	6.3	23.1	M
M24	T	7.7	2.1	2.4	55.9	0.1	<loq	0.3	2.1	4.3	0.1	<loq	0.9	<loq	1.5	0.1	8.9	13.0	M
M25	T	9.0	1.8	1.7	51.3	<loq	<loq	0.7	1.9	2.7	0.1	<loq	0.6	<loq	2.6	0.1	7.6	18.7	M
M26	B	10.4	1.8	1.8	59.1	0.1	<loq	0.5	1.6	4.2	0.1	<loq	1.5	0.5	<loq	<loq	5.9	11.5	M
M27	T	8.2	1.8	1.5	50.1	<loq	<loq	0.6	1.9	2.8	0.1	<loq	0.6	<loq	2.7	<loq	7.5	21.3	M
P3	B	6.6	1.8	3.7	57.5	0.2	<loq	0.3	2.7	5.2	0.1	<loq	2.5	0.6	<loq	0.1	3.7	14.1	M
P14	trans	6.8	1.5	3.6	61.2	0.2	<loq	0.4	2.2	2.9	0.4	<loq	0.7	<loq	0.5	<loq	6.7	12.5	M
P15	B	7.8	2.4	1.9	54.3	0.1	<loq	0.5	1.2	4.2	0.1	<loq	1.6	0.6	0.3	<loq	7.5	16.2	M
P16	B	8.9	2.0	3.1	64.0	0.2	<loq	0.4	2.0	3.1	0.5	0.1	1.6	0.6	<loq	<loq	4.5	8.2	M
P17	T	6.9	2.3	1.9	52.0	<loq	<loq	0.7	2.1	4.2	0.1	0.1	1.2	0.1	2.0	0.1	6.2	19.2	M
V2	trans	0.3	0.4	5.5	31.9	<loq	<loq	0.2	0.5	0.9	0.1	<loq	0.5	0.1	0.4	0.1	<loq	56.1	L
V4	G	0.4	0.5	5.0	40.4	<loq	<loq	0.1	1.6	1.6	<loq	<loq	0.8	0.1	1.4	<loq	<loq	44.9	L
V3	B	12.4	4.0	1.9	69.0	0.3	<loq	0.5	2.4	4.5	0.1	<loq	1.9	0.6	0.4	<loq	0.3	1.2	A
V7	G	0.8	0.3	4.0	24.0	<loq	<loq	0.2	1.0	1.1	0.1	0.1	0.8	<loq	2.1	<loq	<loq	62.3	L
V8	trans	0.2	0.2	1.0	32.2	<loq	<loq	0.1	0.3	0.5	0.1	<loq	0.6	0.2	0.1	<loq	<loq	61.1	L

Table 9. Main oxide wt% averages with standard deviation for the mixed lead alkaline glazes (this study).

Sample	Na ₂ O	MgO	Al ₂ O ₃	SiO ₂	K ₂ O	CaO	Fe ₂ O ₃	PbO
Average (N = 21)	7.5	2.0	2.4	54.9	2.1	3.8	1.3	16.4
Standard Dev.	1.7	0.3	0.8	4.6	0.6	0.8	0.5	5.3

3.4. Glaze Opacity and Colour

The analysed fragments had both opaque and transparent glazes. The most common technique for opacification is the addition of tin oxide in the form of cassiterite, as numerous studies have shown [13,18,32,33]. The glazes from the analysed samples can be discriminated by their tin and lead content (Figure 6) depending on colour and transparency. The high lead-containing glazes are always transparent.

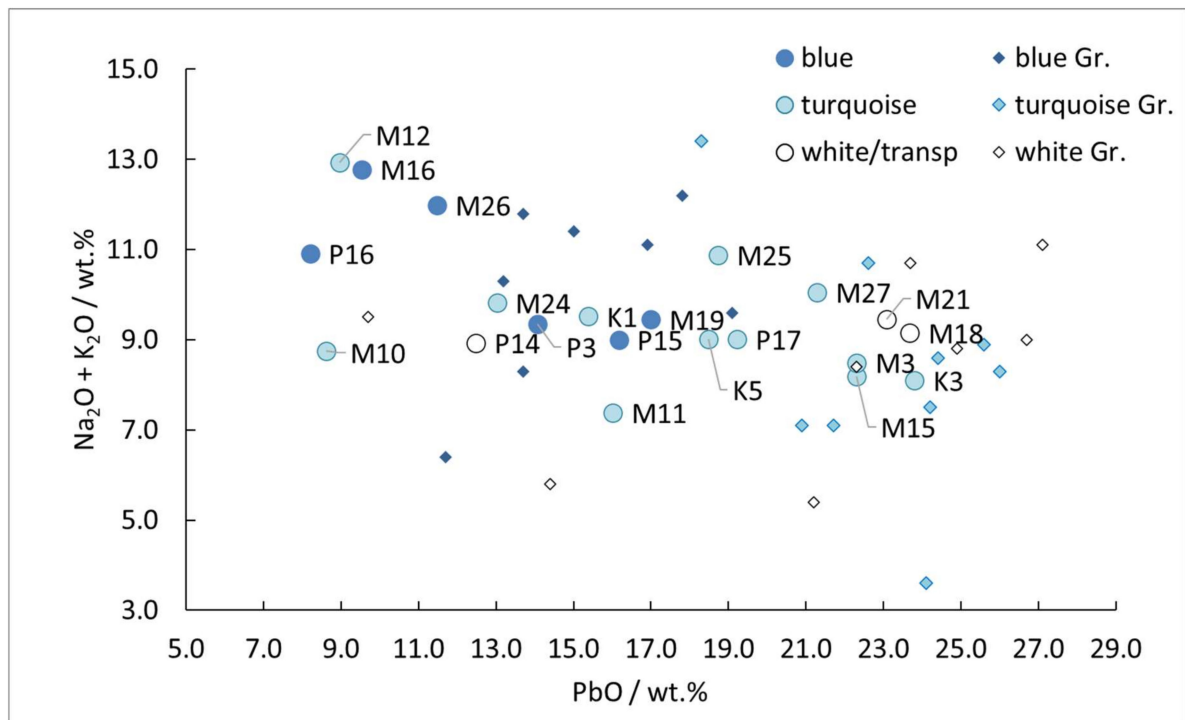


Figure 5. Scatter plot of the SEM/EDX results of glazes with mixed lead alkaline composition. “Gr”: analysis by Gradmann.

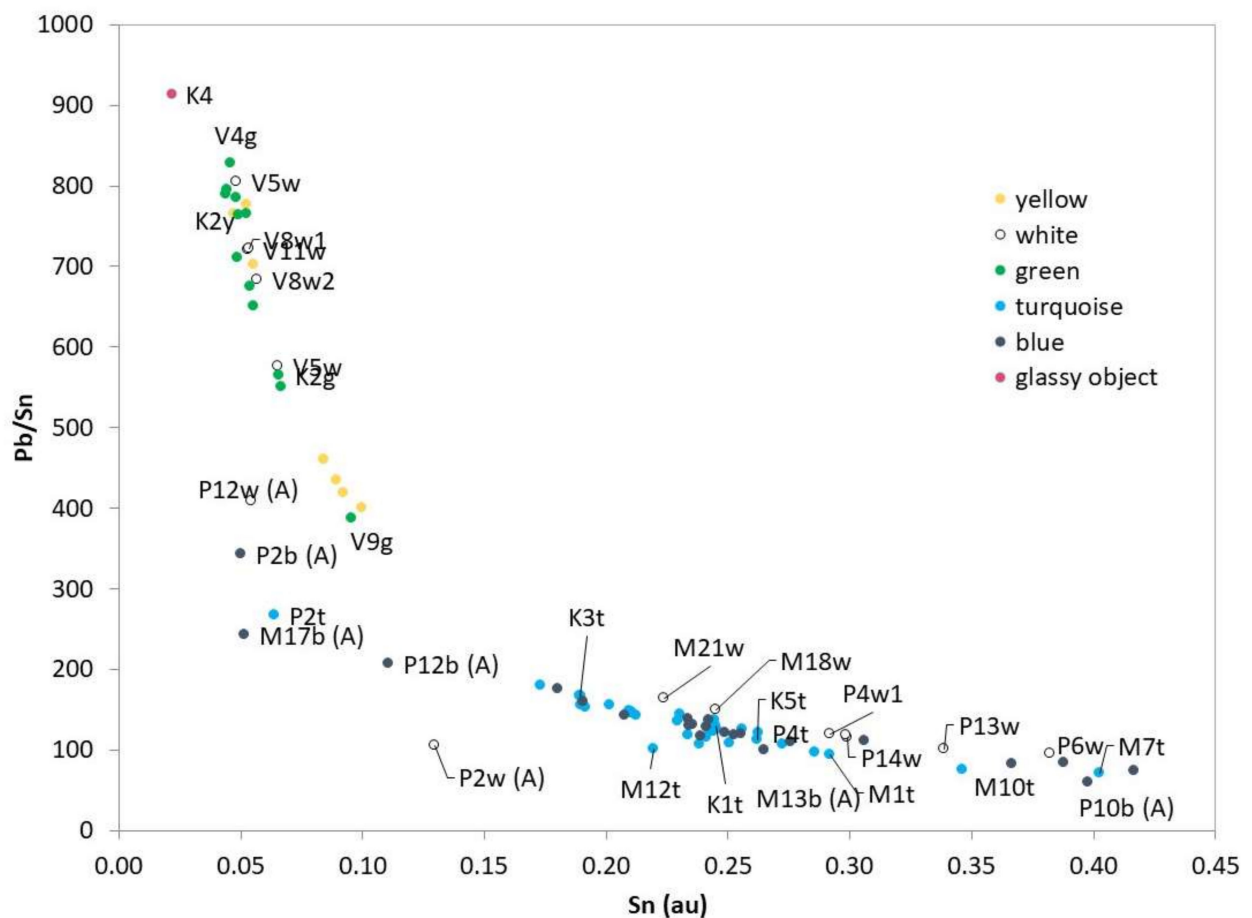


Figure 6. Scatter plot of XRF counts in arbitrary units of tin against the lead/tin ratio.

The transparent lead glazes of vessels form a group in the top left corner of the plot, with high lead and low Sn. These glazes are green, yellow, and colourless, located between the data points V4g and V9g. For these vessels, the transparent coloured or colourless glaze was applied on a white slip. Most of the yellow lead glazes contained more Sn than the green or white ones. The yellow colour was achieved by lead stannate PbSnO_3 crystals in the glassy matrix, which are stable up to about 750 °C in a lead glaze [34]. Above this temperature, PbSnO_3 starts disintegrating into SnO_2 . The firing temperature for the vessels with a yellow glaze would have to be below 800 °C, and is therefore lower than the firing temperature of the mixed glaze of the tiles (820 °C to 1010 °C) [35].

The mixed lead-alkali glazes of the tiles are opaque and mainly coloured in blue, turquoise, or white. In general, most tin-opacified glazes are lead-containing glazes, since SnO_2 crystals were either produced using a lead-containing precursor or precipitated in the glaze during high-temperature firings above 800 °C, when lead stannate dissolved and the tin recrystallized as cassiterite [14,34]. The same studies pointed out that opacification works most effectively within mixed lead-alkali glazes, which is the glaze type used on most tiles analysed in this study.

Only two of the five alkali glazes were opaque: the blue P10b (ISL4) and M13b (TS807). Given the Sn content, opacification seems to originate from cassiterite. The three other alkali glazes (blue M17b, blue P12b, and white P2w) had less tin and were transparent. Figure 6 shows that the transparent alkaline glazes plotted slightly apart from the other glazes with lower lead and tin signals.

The results from residual glazes found on kiln material, and possibly a waster, are interesting since they allow for the identification of locally applied glaze types. The turquoise glazes on K1 (I. 13/69.51 b7), K3 (I. 13/69.51), and K5 (I. 13/69.51 a 00.4) were made with a mixed lead-alkali composition, similar to the one used on tiles. Two other glazes, the green K2g and yellow K2y, were lead glazes (Figures 1 and 6), which had a high similarity with the composition of the lead glazes applied on the vessels.

Most colours are obtained by metal ions dissolved in the glassy matrix. The principal ions used are copper and cobalt (Figure 7). Copper, which can be responsible for light blue to green hues, is present in almost all glazes, either in large amounts or just as a trace. If alkali components or tin are present in significant quantities, copper will give a bluish to turquoise shade, whereas it will turn green in high lead glazes [22,31,35]. The quantitative SEM/EDX results on turquoise and green glazes are given in Table 8 (12 turquoise mixed lead alkaline glazes and two green lead glazes). The Co blue glaze had an elevated As and Fe content compared to the average of the glazes. This suggests that the Co source contained As and Fe as accompanying elements (Figure 8). The traces of Ni and Zn in the blue glaze can be neglected. The Co ore from the mine in Kashan studied by Matin and Pollard showed similar characteristics and is very likely to be the Co source for the colourant of the analysed blue glazes [36].

3.5. Onglaze Decoration

Clay and stonepaste tiles with flat or raised surfaces are decorated with mono- and polychromatic designs. Only the stonepaste tiles are additionally decorated with more elaborate techniques such as lustre (group III), lajvardina (group IIC), and on- and underglaze (group IID) decorations. Lajvardina glazes and on- and under-glaze techniques have been studied, focussing on the minerals used for the onglaze decoration (Table 10).

For the white onglaze decoration of samples P12 (ISL30) and P2 (TS15), cassiterite (SnO_2), used as opacifier in glazes, was identified by Raman spectroscopy (Figure 9).

On P12 (ISL30), a signal was detected at 138 cm^{-1} , k which is possibly associated with the presence of a lead-tin yellow. This compound could have formed from the Pb in the glaze or from Pb that remained as contamination from the production of cassiterite. However, the amount of lead-tin yellow seems to be too insignificant to affect the colour of the glaze. On sample P2 (TS15), quartz and a signal at 479 cm^{-1} , possibly indicating further silicates that were not identifiable, were found in addition to the cassiterite. The white

decorations of samples P11 (ISL2), P15 (TS20), and P3 (TS16) were also analysed. Tin was detected by XRF; Raman spectroscopy, however, could not identify the opacifier.

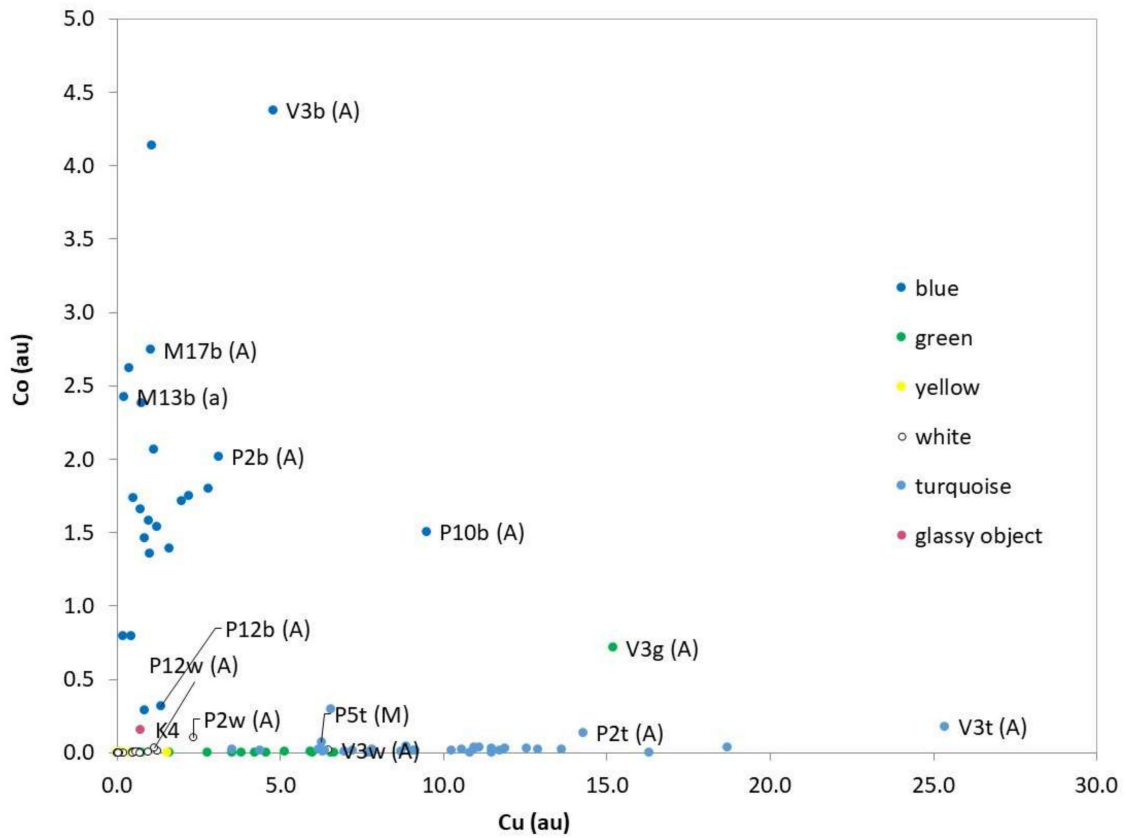


Figure 7. Scatter plot of cobalt against copper as counts obtained by XRF in arbitrary units.

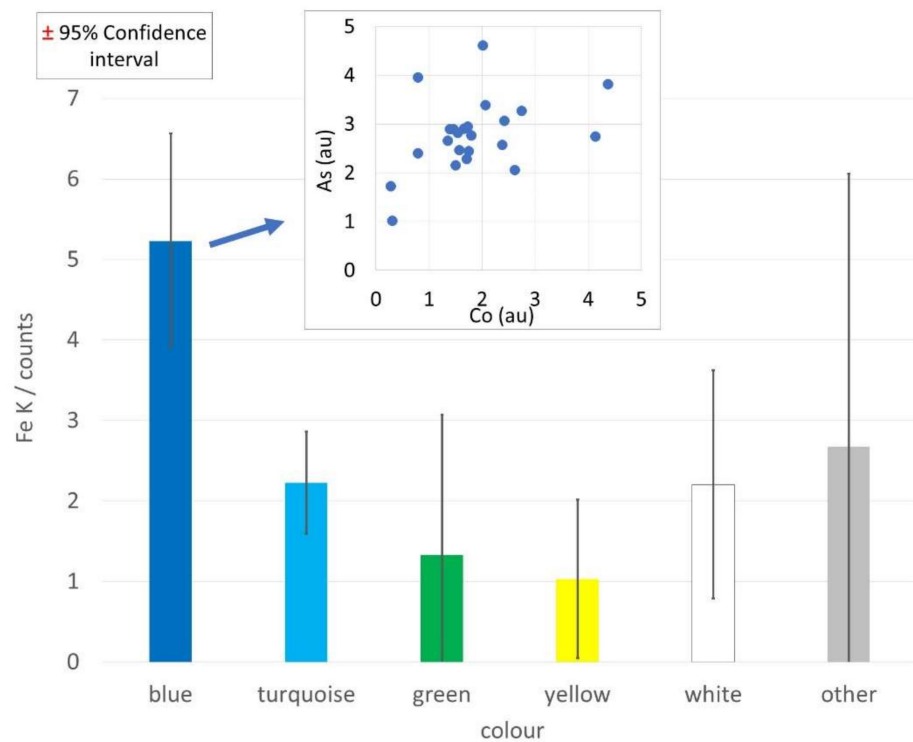


Figure 8. XRF counts of iron for blue, compared to the other glaze colours obtained. Scatter plot of Co against, as in blue glazes (insert), both in arbitrary units.

The XRF analyses showed that all black decorations contained iron and chromium, but no manganese, indicating the sole use of black-iron-chromium pigments. This pigment is frequently found in underglaze-painted Iranian ceramics up to the 19th century. Studies of early Islamic ceramic from Nishapur attest to the use of iron and manganese pigments next to chromium [20,37,38]. Raman spectra from the black colour measured on P2 (TS15/IID), P3 (TS16/IIC), P5 (TS22/IIC), P6 (TS23/IIC), and P12 (ISL30/IID) were quite similar, with an intense band around 673–680 cm^{-1} and a fainter signal around 544–550 cm^{-1} . In this area, the Raman spectra of magnetite $\text{Fe}^{\text{II}}\text{Fe}^{\text{III}}_2\text{O}_4$ and chromite $\text{Fe}^{\text{II}}\text{Cr}^{\text{III}}_2\text{O}_4$ had overlapping bands. Therefore, an unambiguous identification of magnetite and chromite by Raman spectroscopy was difficult. The presence of both compounds in varying proportions could cause variations in the maxima position that were observed in the sample spectra in the range between 662 cm^{-1} and 684 cm^{-1} . A similar mixing was observed in earlier underglaze-painted wares [38]. In the spectra of P14 (TS09/IID), a compound causing the maximum of 703 cm^{-1} could not be identified. XRF showed that a trace of Zn was present in the black of P14.

Strong iron XRF signals were obtained from the brown-red decoration, and the presence of hematite Fe_2O_3 as the colouring agent was confirmed by Raman spectroscopy. The most intense hematite signals (220 cm^{-1} and 285 cm^{-1}) were present in all analysed brown/red spots (P2/TS15, P3/TS16, P5/TS22, P6/TS23, P11/ISL2, P12/ISL30, P14/TS09, and P15/TS20). Some of the signals were slightly shifted and broadened, probably partly due to the reaction of the crystals with the glaze.

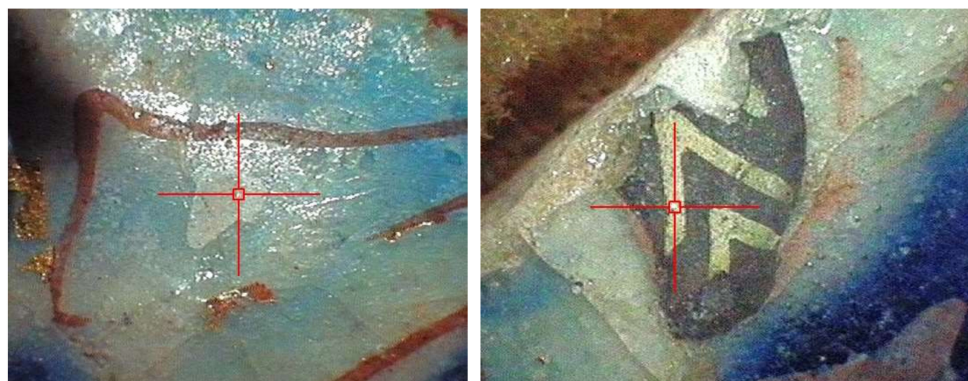


Figure 9. Details of XRF analyses. (Left) White onglaze decoration on P2 (TS15). (Right) Yellow on a black decoration on P12 (ISL30).

Table 10. Results of the analysis of onglaze decoration.

Sample/Object	Group	White		Yellow		Black		Red/Brownish	
		Raman	XRF	Raman	XRF	Raman	XRF	Raman	XRF
P2 (TS15)	IID4	Cassiterite, possibly quartz + other silicates	Sn, Si	Cassiterite, lead chromate, lead tin-yellow	Sn, Pb, Cr	Magnetite/chromite	Fe, Mn	Hematite	Fe
P3 (TS16)	IIC8b	No ident.	Sn			Magnetite/chromite	Fe, Mn	Hematite	Fe
P5 (TS22/IIC)	IIC8b					Magnetite/chromite	Fe, Mn	Hematite	Fe
P6 (TS23/IIC)	IIC					Magnetite/chromite	Fe, Mn	Hematite	Fe
P11 (ISL2)	IIC3	No ident.	Sn					Hematite	Fe
P12 (ISL30)	IID	Cassiterite; (lead-tin yellow)	Sn, (Pb)	Cassiterite, lead chromate, (lead tin-yellow)	Sn, Pb, Cr	Magnetite/chromite	Fe, Mn	Hematite	Fe
P14 (TS09)	IID3c						Fe, Mn, Zn	Hematite	Fe
P15 (TS20)	IIC8b	Not ident.	Sn					Hematite	Fe

The colour yellow was found on the black decoration on two samples: P12/ISL30 and P2/TS15 (Figure 9). Several Raman signals were identified. Cassiterite at 631 cm^{-1} , showed a weak signal at 140 cm^{-1} , probably indicating lead tin-yellow type II ($\text{PbSn}_{1-x}\text{Si}_x\text{O}_3$) and two broad peaks at 358 cm^{-1} and 837 cm^{-1} indicating PbCrO_4 , the pigment lead chromate. Although lead chromate as a pigment was not manufactured until the 19th century [39,40], it has been suggested that the compound may form during firing through a

reaction between chromite and the lead from the glaze [38]. In this case, the chromite in the black beneath the yellow was the source of the Cr, whereas the Pb may have been applied with the cassiterite or was provided by the glaze. However, the glaze is unlikely to be the source of the lead, since it was analysed as an alkaline glaze. Curiously, the yellow was found only on chromium-containing black, leading to the speculation that the formation of the lead chromate was intentional.

4. Conclusions

The samples were classified into compositional groups based on their bodies and glazes: clay or stonepaste for the fabric; alkali, lead, or mixed lead alkali for the glazes. In all cases, except one, the chemical analysis confirmed the macroscopic classification into group I (clay) and group II or III (stonepaste). The visual grouping was confirmed by non-destructive μ -XRF analysis, combined with statistical analyses. This analytical approach is hence suitable for the investigation and categorisation of the remaining large number of tiles in the collection and further studies.

The stonepaste group analysed by SEM/EDX consisted of 20 tiles and one vessel. The compositional group ranged from 72 wt% to 85 wt% in SiO_2 content, which could indicate technological differences within the stonepaste group. In addition to the range of the SiO_2 content, the differences in other elements such as Na_2O_3 and Al_2O_3 might suggest that the production of stonepaste bodies followed slightly varying technologies (e.g., in the quantity of clay added to the mixture). The microstructure of the studied stonepaste ceramics was very similar. Only some variation in the size and shape of the quartz particles was observed. The 'glass' used to produce the stonepaste contained some Pb and Sn, which probably indicates the use of glaze material instead of glass as a "binder" between the quartz particles. The attribution of the stonepaste to a geographical production region was not possible.

The remaining tiles, technical ceramics, and vessels were produced with clay bodies of calcareous clay with around 10 wt% CaO. A closer correlation between the tiles and technical ceramics was obtained for tiles with a content of 5.5 wt% to 9 wt% Fe_2O_3 and 50 wt% to 55 wt% SiO_2 . Clay tiles with less than 5 wt% Fe_2O_3 seemed slightly different in composition, with higher SiO_2 (M14 to M3 in Figure 3).

None of the studied tiles had a lead glaze, only alkaline or mixed lead alkaline glazes were found. The yellow and green lead glazes found on the vessel sherds were not used on tiles. The tiles had almost exclusively mixed lead alkaline glazes, and turquoise, blue, or white were the dominant hues among the analysed fragments. This high frequency of lead alkaline glaze is not paralleled in southern Iran production as Kaczmarczyk's data of production from the 12th to 14th centuries in Susa suggest. However, it has been noted that tiles with the same type of decoration may have different glaze types, despite a similar appearance: for example, in group IID, the blue glaze of P2 (TS15) was alkali and that of P14 (TS09) was mixed (see Supplementary Materials).

The results of the glaze analysis of the technical ceramics were extremely informative. Both lead and mixed glazes were identified on the kiln furniture. Although not necessarily contemporary with the tile production, since the dating of technical ceramics has not been established, the results indicate that at least two types of glazes were produced on site. The colours and composition of the glaze droplets were close to the studied green and yellow lead glazes of the vessels and the turquoise, blue mixed lead alkaline glazes of the tiles (PbO content of 15 wt% to 25 wt%). The lack of evidence concerning alkali glazes might indicate that they were not produced locally or in small quantities.

As for the glazes, the clay bodies showed differences to productions from the region of southern Iran (such as Susa, Siraf, or Sirjan). In addition, imports from Mesopotamia or the Levant can be excluded because the clay compositions did not match with the clay bodies from Takht-e Soleyman. The clay composition from Takht-e Soleyman showed similarities to clay bodies previously analysed from north-western Iran, Nishapur, and Merv. Thus, the elemental analysis by SEM/EDX narrows down the production to northern Iran or

Central Asia. A better differentiation of these wares by SEM/EDX analysis seems to be currently impossible due to the similarity of their elemental composition and lack of references.

Although an accurate provenance or/and workshop attribution was not possible, the combination of the interpretation of glaze and body compositions provides some clues. For example, objects of the macroscopic/stylistic group IA (moulded clay tiles) with turquoise and alkaline-lead mixed glazes might have been produced locally, since the results were comparable with those of the four technical ceramic fragments, provided they are contemporaneous. Analysed examples from this subgroup were M15 and P17. Further analyses are required to confirm and extend the interpretations presented here.

Supplementary Materials: The following are available online at <https://www.mdpi.com/article/10.3390/min12020158/s1>, Table S1: analyses of Glass Standard A from the Corning Museum. Table S2: analyses of Glass Standard B from the Corning Museum. Table S3: analyses of Glass Standard C from the Corning Museum. Table S4: Composition in oxide wt% for the glazes of samples ISL1 (P17). Table S5: Composition in oxide wt% for the glazes of samples ISL7 (M21). Table S6: analysis of the ceramic body by SEM/EDX given in wt%. Table S7: analysis of the glazes by SEM/EDX given in wt%, summarized by colour and ceramic paste. Figure S1: SEM picture of the turquoise glaze of sample P17.

Author Contributions: Conceptualisation, U.F., K.K. and S.R.; Methodology, S.R.; Formal analysis, S.R.; Investigation, A.D. and S.R.; Writing—investigation report and original draft preparation, A.D. and S.R.; Writing—review and editing, S.R., A.D., K.K. and U.F. All authors have read and agreed to the published version of the manuscript.

Funding: A.D. carried out the research during an Erasmus+ placement at Rathgen-Forschungslabor and was supported by the EU. No other external funding was received for this research.

Data Availability Statement: Data is contained within the article or supplementary material. Further data can be made available on qualified request from the corresponding author.

Acknowledgments: The authors are grateful to Ina Reiche and Stefan Simon as directors of the Rathgen-Forschungslabor for supporting this project. SR is grateful to Parvis Holakooei for discussions about the ceramics and the site of Takht-e Soleyman.

Conflicts of Interest: The authors declare no conflict of interest.

References

1. Blair, S.S.; Bloom, J.M. *The Art and Architecture of Islam 1250–1800*; Yale University Press: London, UK, 1996; ISBN 0-300-06465-9.
2. Masuya, T. *The Ilkhanid Phase of Takht-i Suleiman*; New York University, Graduate School of Arts and Science, Institute of Fine Arts: New York, NY, USA, 1997.
3. Young, T.C.; Stronach, D.; Schippmann, K.; Huff, D.; Masson, V.M.; Hillenbrand, R.; Pugachenkova, G.A.; Rtveldze, E.V.; Pogrebova, M.N. Archeology. In *Encyclopaedia Iranica Online*; Brill: New York, NY, USA, 1986.
4. Huff, D. Takht-i Suleiman. Sasanian Fire Sanctuary and Mongolian Palace. In *Persia's Ancient Splendour. Mining, Handicraft and Archaeology*; Stoeller, T., Slotta, R., Vatandoust, A., Eds.; Exhibition Catalogue Katalog Deutsches Bergbau-Museum Bochum: Bochum, Germany, 2004; pp. 462–471.
5. Naumann, R. *Die Ruinen von Tacht-e Suleiman und Zendan-e Suleiman und Umgebung. Führer zu Archäologischen Plätzen in Iran 2*; Reimer: Berlin, Germany, 1977.
6. Huff, D. TAKT-E SOLAYMÂN. In *Encyclopaedia Iranica Online*; Brill: New York, NY, USA, 2002.
7. Franke, U. *Die Baukeramik Vom Tacht-i Suleiman, Azerbaijan, Iran. Magisterarbeit*; George-August-Universität: Göttingen, Germany, 1979.
8. Franke, U.; Huff, D.; Masuya, T. The Ilkhanid Architecture and Its Tile Decoration at Takht-e Soleyman, Iran. 2023; *in press*.
9. Porter, V. *Islamic Tiles*; British Museum Press: London, UK, 1995.
10. DeGeorge, G.; Porter, Y. *The Art of the Islamic Tile*; Flammarion: Paris, France, 2002; ISBN 2-08-010876-X.
11. Masuya, T. Ilkhanid Courtly Life. In *The Legacy of Genghis Khan: Courtly Art and Culture in Western Asia, 1256–1353*; Yale University Press: New York, NY, USA; New Haven, CT, USA; London, UK, 2002; pp. 74–103. ISBN 1-58839-071-3.
12. Gradmann, R. *Analysis of Historical Islamic Glazes and the Development of a Substitution Material*; Universität Würzburg: Würzburg, Germany, 2016.
13. Tite, M.S.; Salter, C. Report on the Examination of Islamic Cuerda Seca Tiles from the Collections of the Victoria and Albert Museum. In *And Diverse Are Their Hues: Color in Islamic Art and Culture*; Bloom, J.M., Blair, S.S., Eds.; Yale University Press: New Haven, CT, USA, 2011; pp. 200–203. ISBN 978-0-300-17572-1.

14. Matin, M.; Tite, M.; Watson, O. On the Origins of Tin-Opacified Ceramic Glazes: New Evidence from Early Islamic Egypt, the Levant, Mesopotamia, Iran, and Central Asia. *J. Archaeol. Sci.* **2018**, *97*, 42–66. [[CrossRef](#)]
15. Osete-Cortina, L.; Doménech-Carbó, M.T.; Doménech, A.; Yusá-Marco, D.J.; Ahmadi, H. Multimethod Analysis of Iranian Ilkhanate Ceramics from the Takht-e Soleyman Palace. *Anal. Bioanal. Chem.* **2010**, *397*, 319–329. [[CrossRef](#)]
16. Hirx, J.; Leona, M.; Meyers, P. Technical Study 2: The Glazed Press-Molded Tiles of Takht-i Sulaiman. In *The Legacy of Genghis Khan: Courtly Art and Culture in Western Asia, 1256-1353*; Metropolitan Museum of Art: New York, NY, USA, 2002; pp. 233–242. ISBN 1-58839-071-3.
17. Tite, M.S. The Technology of Glazed Islamic Ceramics Using Data Collected by the Late Alexander Kaczmarczyk. *Archaeometry* **2011**, *53*, 329–339. [[CrossRef](#)]
18. Al-Saad, Z. Chemical Composition and Manufacturing Technology of a Collection of Various Types of Islamic Glazes Excavated from Jordan. *J. Archaeol. Sci.* **2002**, *29*, 803–810. [[CrossRef](#)]
19. Coentro, S.; Mimoso, J.M.; Lima, A.M.; Silva, A.S.; Pais, A.N.; Muralha, V.S. Multi-Analytical Identification of Pigments and Pigment Mixtures Used in 17th Century Portuguese Azulejos. *J. Eur. Ceram. Soc.* **2012**, *32*, 37–48. [[CrossRef](#)]
20. Mason, R.B. *Shine Like the Sun: Lustre-Painted and Associated Pottery from the Medieval Middle East*; Mazda Pub: Costa Mesa, CA, USA, 2004; Volume 12, ISBN 1-56859-096-2.
21. Watson, O. *Ceramics from Islamic Lands*; Thames & Hudson: London, UK, 2004; ISBN 0-500-97629-5.
22. Allan, J.W. Abū'l-Qāsim's Treatise on Ceramics. *Iran* **1973**, *11*, 111–120. [[CrossRef](#)]
23. Tite, M.S.; Wolf, S.; Mason, R.B. The Technological Development of Stonepaste Ceramics from the Islamic Middle East. *J. Archaeol. Sci.* **2011**, *38*, 570–580. [[CrossRef](#)]
24. Matin, M. On the Technology of Medieval Islamic Ceramics: A Study of Two Persian Manuscripts. In *Ceramics of Iran: Islamic Pottery from the Sarikhani Collection*; Yale University Press: London, UK, 2020; pp. 459–487. ISBN 0-300-25428-8.
25. Watson, O. Medieval Wares. In *Ceramics of Iran: Islamic Pottery from the Sarikhani Collection*; Yale University Press: London, UK, 2020; pp. 146–345. ISBN 0-300-25428-8.
26. Schneider, G.; Daszkiewicz, M. Imported and Local Fimalampen in Aquileia. Chemical Analyses by WD-XRF. *Aquileia Nostra* **2011**, *82*, 261–282.
27. Naumann, R. *Brennöfen Für Glasurkeramik*; Ernst Wasmuth: Tübingen, Germany, 1971.
28. Brill, R.H. Appendix D: Reference Glasses. In *Chemical Analyses of Early Glasses*; Corning: New York, NY, USA, 1999; Volume 2, p. 544.
29. Chabanne, D.; Aucouturier, M.; Bouquillon, A.; Darque-Ceretti, E.; Makariou, S.; Dectot, X.; Fay-Hallé, A.; Miroudot, D. Ceramics with Metallic Lustre Decoration. A Detailed Study of Islamic Productions from the 9th Century until the Renaissance. *Matér. Tech.* **2012**, *100*, 47–68. [[CrossRef](#)]
30. Frahm, E. Ceramic Studies Using Portable XRF: From Experimental Tempered Ceramics to Imports and Imitations at Tell Mozan, Syria. *J. Archaeol. Sci.* **2018**, *90*, 12–38. [[CrossRef](#)]
31. Weyl, W.A. *Coloured Glasses*; Reprint from 1999; Society of Glass Technology: Sheffield, UK, 1951.
32. Tite, M.; Pradell, T.; Shortland, A. Discovery, Production and Use of Tin-Based Opacifiers in Glasses, Enamels and Glazes from the Late Iron Age Onwards: A Reassessment. *Archaeometry* **2008**, *50*, 67–84. [[CrossRef](#)]
33. Molera, J.; Vendrell-Saz, M.; Pérez-Arantegui, J. Chemical and Textural Characterization of Tin Glazes in Islamic Ceramics from Eastern Spain. *J. Archaeol. Sci.* **2001**, *28*, 331–340. [[CrossRef](#)]
34. Tite, M.; Watson, O.; Pradell, T.; Matin, M.; Molina, G.; Domoney, K.; Bouquillon, A. Revisiting the Beginnings of Tin-Opacified Islamic Glazes. *J. Archaeol. Sci.* **2015**, *57*, 80–91. [[CrossRef](#)]
35. Gradmann, R.; Berthold, C.; Schüssler, U. Composition and Colouring Agents of Historical Islamic Glazes Measured with EPMA and μ -XRD2. *Eur. J. Mineral.* **2015**, *27*, 325–335. [[CrossRef](#)]
36. Matin, M.; Pollard, A.M. From Ore to Pigment: A Description of the Minerals and an Experimental Study of Cobalt Ore Processing from the Kāshān Mine, Iran: From Ore to Pigment: The Cobalt Minerals and Ore Processing from the Kāshān Mine, Iran. *Archaeometry* **2017**, *59*, 731–746. [[CrossRef](#)]
37. Reiche, I.; Röhrs, S.; Salomon, J.; Kanngießer, B.; Höhn, Y.; Malzer, W.; Voigt, F. Development of a Nondestructive Method for Underglaze Painted Tiles—Demonstrated by the Analysis of Persian Objects from the Nineteenth Century. *Anal. Bioanal. Chem.* **2009**, *393*, 1025–1041. [[CrossRef](#)] [[PubMed](#)]
38. Holakooei, P.; de Lapérouse, J.-F.; Carò, F.; Röhrs, S.; Franke, U.; Müller-Wiener, M.; Reiche, I. Non-Invasive Scientific Studies on the Provenance and Technology of Early Islamic Ceramics from Afrasiyab and Nishapur. *J. Archaeol. Sci. Rep.* **2019**, *24*, 759–772. [[CrossRef](#)]
39. Kühn, H.; Curran, M. Chrome Yellow and Other Chromate Pigments. In *Artists' Pigments; A Handbook of Their History and Characteristics*; Feller, R.L., Ed.; Cambridge University Press: Cambridge, UK, 1986; Volume 1, pp. 187–217. ISBN 0-521-30374-5.
40. Bell, I.M.; Clark, R.J.; Gibbs, P.J. Raman Spectroscopic Library of Natural and Synthetic Pigments (Pre- \approx 1850 AD). *Spectrochim. Acta. A. Mol. Biomol. Spectrosc.* **1997**, *53*, 2159–2179. [[CrossRef](#)]